J Infrared Milli Terahz Waves (2017) 38:1215–1231
DOI 10.1007/s10762-017-0414-x

ALMA Band 1 Optics (35–50 GHz): Tolerance Analysis, Effect of Cryostat Infrared Filters and Cold Beam Measurements

A . Gonzalez[1] · V. Tapia[2] · R. Finger[2] · C.-D. Huang[3] · S. Asayama[1] · Y.-D. Huang[4]

Received: 26 April 2017 / Accepted: 20 June 2017 /
Published online: 1 July 2017

Abstract The Atacama Large Millimeter/Sub-millimeter Array (ALMA) is currently the largest (sub-)mm wave telescope in the world and will be used for astronomical observations in all atmospheric windows from 35 to 950 GHz when completed. The ALMA band 1 (35–50 GHz) receiver will be used for the longest wavelength observations with ALMA. Because of the longer wavelength, the size of optics and waveguide components will be larger than for other ALMA bands. In addition, all components will be placed inside the ALMA cryostat in each antenna, which will impose severe mechanical constraints on the size and position of receiver optics components. Due to these constraints, the designs of the corrugated feed horn and lens optics are highly optimized to comply with the stringent ALMA optical requirements. In this paper, we perform several tolerance analyses to check the impact of fabrication errors in such an optimized design. Secondly, we analyze the effects of operating this optics inside the ALMA cryostat, in particular the effects of having the cryostat IR filters placed next to the band 1 feed horn aperture, with the consequent near-field effects. Finally, we report on beam measurements performed on the first three ALMA band 1 receivers inside test cryostats, which satisfy ALMA specifications. In these measurements, we can clearly observe the effects of fabrication tolerances and IR filter effects on prototype receiver performance.

Keywords Quasi-optics · Radio astronomy · ALMA · mm-wave · Tolerance analysis · Cryogenic receiver · Dielectric lens · Corrugated horn · mm-wave measurements

✉ A . Gonzalez
Alvaro.Gonzalez@nao.ac.jp

[1] National Astronomical Observatory of Japan, Tokyo, Japan

[2] Universidad de Chile, Santiago, Chile

[3] National Chung-Shang Institute of Science and Technology, Taichung, Taiwan

[4] Academia Sinica Institute of Astronomy and Astrophysics, Taipei, Taiwan

1 Introduction

The Atacama Large Millimeter/Sub-millimeter Array (ALMA) is the largest mm/sub-mm wave telescope in the world and has been built as a collaboration among Europe, North America, East Asia, and Chile. The telescope is located at 5000 m altitude in the Atacama Desert in northern Chile, where superb atmospheric conditions make observations possible from 35 GHz up to at least 950 GHz [1]. Such a large frequency coverage has been achieved with ten different receivers covering different frequency ranges. The telescope is composed of 54 12-m antennas and 12 7-m antennas, each of them equipped with a cryostat to cool down the ten different receivers for each of the ALMA bands to cryogenic temperatures for state-of-the-art sensitivity, close to physical limits. The ALMA band 1 receivers are used to observe the longest wavelengths in ALMA, with frequencies in the 35–50 GHz range [2]. This implies that the size of components in the front-end is larger than for other ALMA bands. This imposes serious mechanical constraints in the size and position of optical components. On the one hand, components will require highly compact and optimized designs to achieve the required performance with a limited size. On the other hand, the feed horn will be placed next to the cryostat infrared filters, which will degrade the feed performance due to mutual coupling effects. In addition, the size of the cryostat apertures in the optical path, between the Cassegrain secondary mirror and the receiver, is small compared to the incoming beam, which causes considerable beam truncation. Finally, the fractional bandwidth of band 1 is about 36%, which is the largest in any of the original ALMA bands. All these considerations make the design of the band 1 receiver and optics an engineering challenge.

Different optical configurations have been studied for the ALMA band 1 receiver optics [3–5] over the years. The final optical design, fully compliant with ALMA requirements, was firstly presented in [4]. The final summary of the design and room-temperature performance of the band 1 receiver optics was recently published in [5]. It consists of a compact spline-profile corrugated horn attached to the receiver and an HDPE dielectric lens which acts as cryostat window and matches the incoming beam from the Cassegrain antenna to the feed horn beam. A schematic of the optics is shown later in Fig. 7. In this paper, we perform some critical analyses to understand how fabrication errors and operation within the ALMA cryostat will affect the performance of such an optimized antenna design. Firstly, we present different tolerance analyses on individual receiver optics components and on the full optics. Secondly, we analyze the effect of cryostat IR filters on optical performance. Finally, we present beam measurement results performed with the optics assembled in the first three prototype ALMA band 1 receivers cooled down to cryogenic temperature inside a test cryostat. All these studies are the key to understanding the measured performance in cryogenically cooled receivers and are of interest for combinations of feed horn and dielectric lens at mm-wave frequencies, especially when operated at cryogenic temperature or under vacuum conditions.

2 Tolerance Analysis

The ALMA band 1 optics are a highly optimized design due to stringent requirements and mechanical constraints. Any fabrication and assembly errors will presumably have an impact on performance. In order to quantify the effects of tolerances on the different components in the optics and on the optics as a whole, three different tolerance analysis have been performed on the baseline band 1 receiver optics design in [5]: a Monte Carlo analysis [6] on the

dimensions of the corrugated feed horn, a parametric analysis on the dimensions of the dielectric lens when illuminated by the nominal feed horn, and a Monte Carlo analysis of the full ALMA band 1 optics. Refer to [5] for detailed values of nominal parameters. Details of each analysis and results are presented in the next sections. These analyses are based on the ideas in [7, 8] and the performed simulations provide full radiation patterns to analyze performance, as opposed to simpler tolerance analyses based on, for example, ray tracing [9].

2.1 Tolerance Analysis of the Corrugated Feed Horn

The ALMA band 1 feed horn, shown in Fig. 1, is a highly optimized profiled corrugated horn. The dimensions of each corrugation have been optimized for minimum size, ease of fabrication, and high-performance (s_{11} <−30 dB, cross-polarization <−35 dB). During production of ALMA band 1 receivers, each receiver will need one corrugated horn. Therefore, 73 units will be required. Fabrication errors in the horn corrugations will have an impact on performance. In particular, the worst values of input return loss (s_{11}) and cross-polarization will increase. These effects have been quantified by means of two different Monte Carlo analyses, for fabrication errors up to 25 and 50 μm.

To implement these tolerance analyses, random errors have been added to the horn nominal dimensions and the resulting models have been analyzed with the Mode-Matching/Method-of-Moments software WaspNet [10]. S-parameters and radiated far fields have been stored and analyzed with MATLAB [11] just after EM simulations. The random errors added to dimensions follow a uniform distribution between ±max errors. The values of errors randomly chosen are 65 variables: 1 for C, 1 for G, and the rest for all the different ri, Ri (see Fig. 1 for a graphical description). The change in C and G will change the value of the corrugation pitch and, consequently, the horn profile. The full analysis is done automatically with a MATLAB function, which takes two input variables: number of horns N to be simulated and maximum error allowed. This function generates the geometries for the N horns, creates the WaspNet simulation files, runs the simulations and automatically analyzes the results and stores the data. WaspNet simulations are run with cutoff frequency of 200 GHz and connection of 70%, which is enough for convergence with Mode-Matching. The full analysis of each horn takes 2 min in our simulation server, with frequency points spaced 1 GHz between 35 and 50 GHz. Two cases have been considered, for maximum errors of 25 and 50 μm. The results of the two analyses are presented in Fig. 2, which shows all the s_{11} and maximum cross-

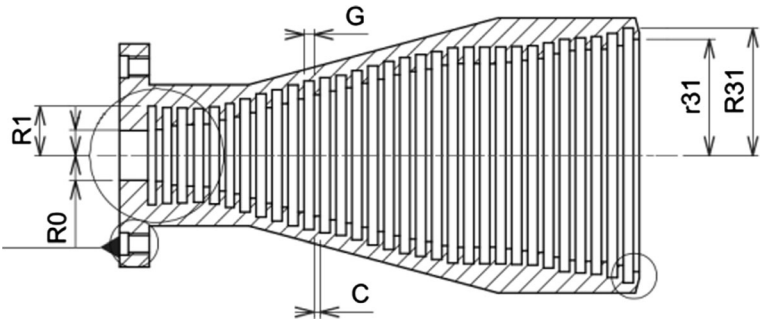

Fig. 1 Drawing of the ALMA band 1 profiled corrugated horn. The horn consists of 31 variable depth corrugations. The width of the first corrugations has also been optimized for better performance

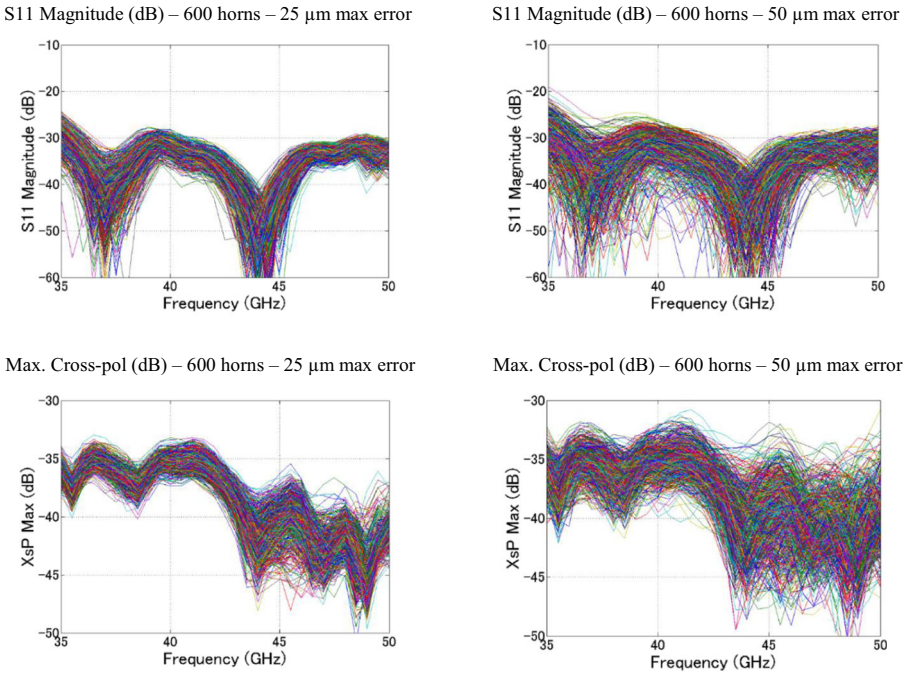

Fig. 2 Results of the Monte Carlo tolerance analyses for the ALMA band 1 corrugated horn

polarization results for 600 horns with maximum fabrication errors of 25 and 50 μm. This number of simulations is low for a parameter space of 65 variables and a careful analysis of statistics is therefore not meaningful in this case. Instead, the particular simulated cases provide a good qualitative assessment of the expected variation in performance.

The worst values of reflection loss and cross-polarization worsen as the maximum allowed error increases. In the case of reflection loss, we can see that the values of s_{11} at the lower part of the band, around 35 GHz, degrade considerably. The worst values for 25 μm maximum errors are around −25 dB, whereas they can be higher than −20 dB for 50 μm maximum errors. Values of −20 dB or worse could have some negative consequences in the total optics reflection loss. With respect to cross-polarization, it stays below –33 dB for maximum errors of 25 μm, whereas worst-case values get closer to −30 dB for maximum errors of 50 μm. In addition, results in the upper part of the band are considerably better for 25 μm than for 50 μm.

In conclusion, it is necessary to keep fabrication errors in the corrugated horn below 25 μm to guarantee good performance of the 73 units to be fabricated. This is a challenging but achievable target with current fabrication technology.

2.2 Parametric Analysis of the Dielectric Lens

A parametric analysis on the dimensions and material properties of the HDPE lens used to match the beams from the corrugated horn and the ALMA Cassegrain antennas is necessary to understand the required tolerances during the production of 73 units, and to assess what parameters have a larger impact on RF performance. In this analysis, one parameter is swept, while all others are kept constant. The corrugated horn in these simulations is also ideal. The

dimensions and lens characteristics which have been modified are lens-horn distance, lens diameter, dielectric constant, central slab thickness, grooves width and depth, and height errors in the steps that create the lens profile. These last errors have been considered in five different areas in the lens: steps 1–10, 11–20, 21–30, 31-end of central hyperbola, and steps in the Fresnel zone. Doing this, we can see how changes in different zones affect performances differently. Electromagnetic simulations have been performed using WaspNet Mode-Matching/Body-Of-Revolution (BOR) Method of Moments hybrid code. Therefore, the only limitation in the analysis is to keep the BOR geometry of the optics. Far fields have then been analyzed with in-house efficiency calculation software. The frequency coverage of the analysis is from 34 to 51 GHz, with 1 GHz frequency spacing. This fine frequency sweep allows to see changes in frequency dependence performances. Figure 3 shows the drawing of the lens for reference.

Results of the parametric analysis on aperture efficiency at the secondary mirror of the Cassegrain antenna are presented in Fig. 4. These results show that performance depends critically on the distance between horn and lens, on the lens diameter, and dielectric constant. The first two dimensions are basically determined by mechanical constraints, as explained in [5]. The lens size and distance cannot be increased due to some other instruments on top of the ALMA cryostat. The distance between lens and horn must be controlled within 1 mm for minimum changes in aperture efficiency. Errors around 2 mm would introduce some degradation at band edges. The other critical parameter is the dielectric constant of the lens material. Changes of 2% in dielectric constant values would bring the aperture efficiency out of specifications. This highlights the need of careful control of the dielectric properties, and monitoring over time to detect the possibility of material aging (which has not been done before for HDPE to the extent of the authors' knowledge). Apart from these parameters, the height of steps and depth of the grooves of the anti-reflection coating will have an impact on performance. In the case of the height of steps, similar errors will have more effect on central steps than on those at the lens edge. The groove width has little impact on performance. These conclusions indicate that tolerances on groove width, and heights on lens edge steps, could be relaxed if necessary to ease fabrication. A maximum error of 50 μm or even larger would still be acceptable for production according to this analysis. Errors in central slab thickness do not have much impact for reasonable error values.

Finally, it is important to mention that in some of the simulated cases, performance seems better than in the nominal case. However, we must keep in mind that the nominal design has been done to be as frequency independent as possible, and it has considered some mechanical constraints slightly relaxed in this analysis. In other cases, the changes in dimensions affect other performances not reported here. For example, a reduction of the AR groove depth will improve the aperture efficiency, due to an improvement in polarization efficiency. However, it

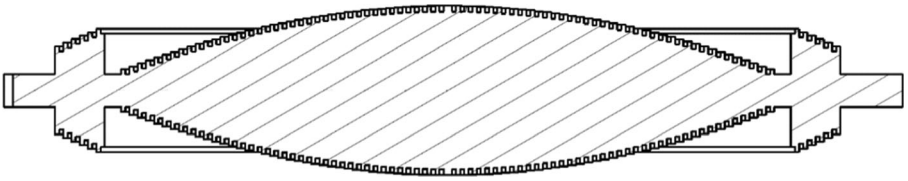

Fig. 3 Drawing of the ALMA band 1 lens. The anti-reflection coating is made of concentric grooves. The lens profile between grooves is composed of flat steps to simplify fabrication

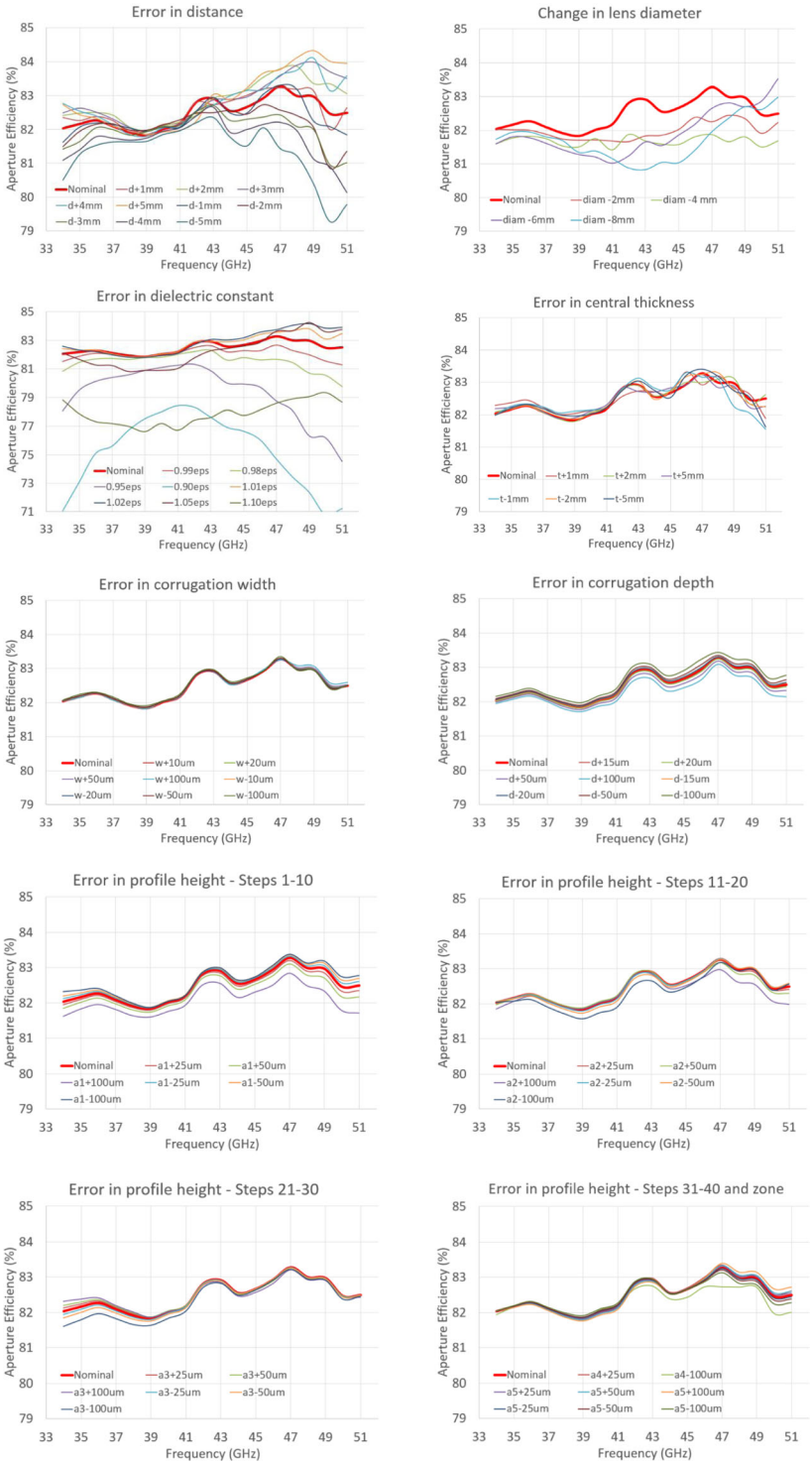

Fig. 4 Results of aperture efficiency calculations for the parametric analysis of the ALMA band 1 lens

also degrades the reflection loss of the lens and can potentially create standing waves and degradation of other receiver performances.

In terms of polarization efficiency, the performance is pretty insensitive to changes, except in the case of changes in dielectric constant or groove depth. These parameters were already important for aperture efficiency and will be therefore carefully controlled during the fabrication of the 73 production units of the ALMA band 1 lens. Figure 5 shows the dependence on these parameters. Two different polarization efficiencies are presented, one integrated on the full radiation pattern and the other integrated on the secondary mirror. The ALMA specification of polarization efficiency >99.5% applies on this latter quantity.

2.3 Monte Carlo Analysis of ALMA Band 1 Optics

After careful consideration of possible fabrication errors in the corrugated horn and dielectric lens, it is necessary to consider the effects on performance of combined effects. To do this, a Monte Carlo analysis considering errors in the horn and lens has been performed. Assembly errors cannot be easily simulated, since the BOR geometry would be lost and simulations would take a considerably longer time. Simulations have been performed on nine frequency points from 35 to 51 GHz, which means one frequency point every 2 GHz. MATLAB has been used to generate all random errors, create WaspNET files, start WaspNET simulations, and analyze results. Each step takes 1 h and 10 min approximately. This has been repeated automatically for a total of 326 simulations, for a total of ~400 h. The applied errors follow uniform distributions with maximum values of ±25 μm for horn corrugation dimensions, and

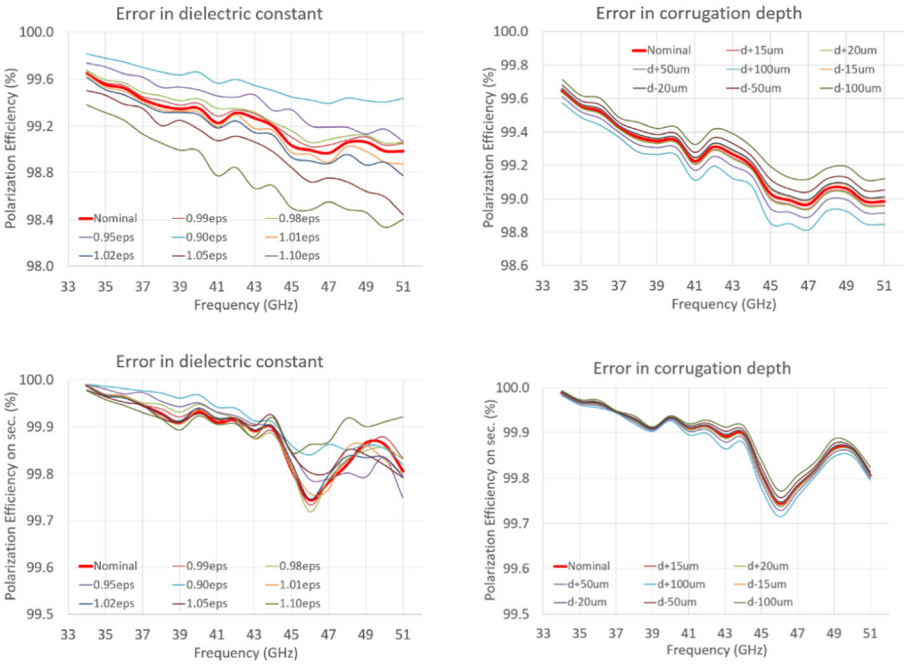

Fig. 5 Changes in polarization efficiency (integrated on the full pattern and on the secondary mirror of the ALMA antenna) for deviations from nominal of dielectric constant and groove depth

±50 μm for lens profile dimensions. The horn model parameters are the same as in Section 2.1, 63 variables for the corrugation radii and 2 variables for the corrugation tooth and slot width. For the lens, nine variables have been used to model errors: distance between horn and lens, dielectric constant, depth and width of grooves, and step heights in groups of 10 steps (1–10, 11–20, 21–30, 31–40, 41–edge of lens). The maximum error values are ±1 mm in distance, ±1% in dielectric constant, and ±50 μm for groove and step dimensions. Results of this analysis in terms of s_{11}, aperture efficiency, and polarization efficiencies (on full pattern and on the secondary mirror of the ALMA antenna) are presented in Fig. 6. As in Section 2.1, the number of simulation is not enough for careful statistical analysis but provide a good qualitative assessment on the impact of tolerances on performance.

Results of the tolerance analysis indicate that all 326 simulations show ALMA compliant performance (aperture efficiency >80%, polarization efficiency on secondary >99.5%). The effect of tolerances on performance creates larger variations at higher frequencies, when the errors are electrically larger. Therefore, there were more cases about to be non-compliant at the higher end of the ALMA band 1. In those cases, performance could be out of specs with the ripples introduced by the effect of IR filters, as explained in Section 3.

3 Effect of the Cryostat Infrared Filters

During operation in the ALMA telescope, the band 1 receiver will be cooled down to cryogenic temperatures inside a cryostat placed in the secondary focus of each ALMA Cassegrain antenna. The operation temperature close to 0 K is achieved progressively in different stages. From room temperature, the stage temperature is reduced to 110 K and then to

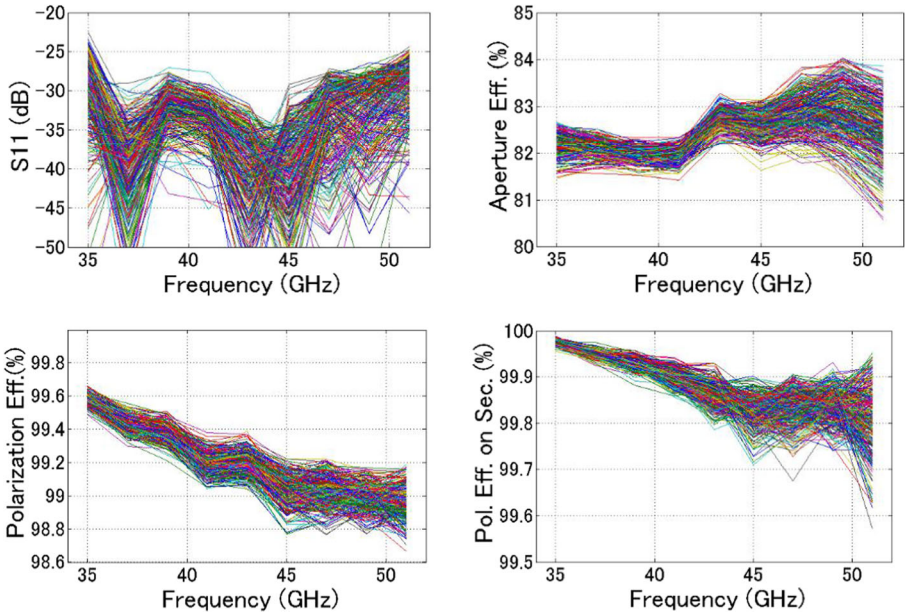

Fig. 6 Results of the Monte Carlo tolerance analysis for the ALMA band 1 optics, considering maximum fabrication errors of 25 μm for the corrugated horn and of 50 μm for the dielectric lens

15 K (and 4 K, in the case of ALMA band 3 to 10, which use superconducting mixers). Between the different stages, there are infrared (IR) filters to reduce the thermal load from the warmer stages into the innermost colder stages. In addition, the apertures in the different shields separating stages cannot be large due to thermal considerations. Therefore, the beam coming from the secondary mirror of the Cassegrain antenna will come into the cryostat through the band 1 lens, which is used as vacuum seal for the cryostat, and through small apertures covered by plastic materials (IR filters) before reaching the band 1 corrugated horn. In the case of band 1, the size of components is comparatively large compared to other bands, due to the longer wavelength. This makes that cryostat shield apertures are electrically small. To avoid excessive truncation, the feed horn has to be placed very close to the first IR filter, which will have negative consequences due to near-field effects. There are two IR filters in the optical path of the ALMA band 1 receiver, at the cryostat 15 and 110 K shields. The 15 K filter is a 3-mm-thick Goretex layer, placed only 5 mm away from the horn aperture. The 110 K filter, made of PTFE, is a 5-mm-thick slab with triangular groove anti-reflection coating on both sides, and it is placed around 31 mm from the horn aperture. The total thickness of the AR layer on one side is 7.651 mm. This situation is depicted in Fig. 7. The first results of the effects of these IR filters on ALMA band 1 optics were reported in [12]. In this paper, we summarize that previous work and extend it with newer results.

3.1 Effect on the Feed Horn Radiation Patterns

The negative effect of IR filters on optics performance was reported for the first time for the ALMA band 4 receiver [13]. At that time, it was found that when the beam passes through the IR filters, it generates magnetic currents on the dielectrics and electric currents on the metal support rims. These currents will radiate and cause mutual impedance coupling effects to the currents on the horn aperture, which determine the radiation properties of the band 1 horn. The effect of the IR filters appears in the radiated field expressions of the horn by means of the admittance seen by the horn at the aperture plane and it will be different for orthogonal linear polarizations. The exact equations have been reported in [13]. The input admittance depends on the relative positions of horn and IR filters, as well as tilt angles, offsets, and material

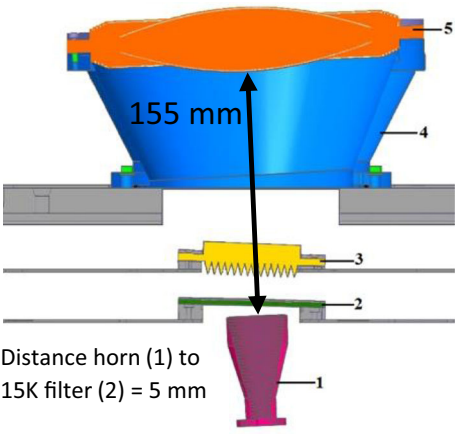

Fig. 7 Cross section of the ALMA band 1 optics installed in the ALMA cryostat. The lens (5) is placed on top of a lens holder (4) which provides the appropriate tilt and distance to the feed horn. The lens acts as cryostat window and holds vacuum. The incoming radiation must go through two IR filters placed on support rims on the 110 K shield (3) and the 15 K shield (2) before finally reaching the band 1 corrugated horn (1)

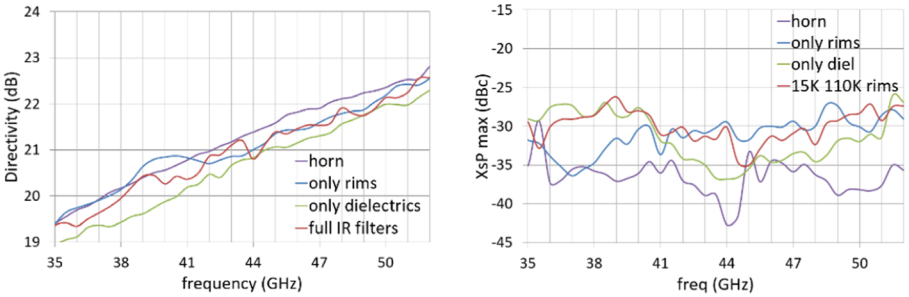

Fig. 8 Directivity and maximum XsP of the equivalent feed horn resulting from different combinations of corrugated horn and IR filters and their rims (with their exact geometry)

properties. The frequency behavior changes very much with small changes in IR filter positions.

In the case of the ALMA band 1 feed horn, the geometry is quite compact and can be simulated by finite elements with HFSS [14] and powerful simulation computers. Results with a fine frequency sweep show the change in co- and cross-polarization feed horn radiation patterns. Figure 8 presents the changes in directivity and maximum cross-polarization for the horn alone, and when loaded with only the metal part of IR filters assembly, only the dielectric layers in the IR filters, and the full IR filter assemblies. The effect of the impedance coupling is a reduction in directivity and an increase in cross-polarization.

3.2 Effects on Aperture and Polarization Efficiencies

The reported changes in feed horn radiation patterns will have an impact on the aperture and polarization efficiencies of the full ALMA band 1 optics. Unfortunately, the lens assembly cannot be added to the previous HFSS simulations for exact calculations due to limitations in computer resources. Instead, it was decided to perform a qualitative analysis using the BOR Method of Moments code in WaspNET. This analysis is approximate because we cannot add two important characteristics of the IR filter geometry: tilt angles and offsets with respect to the optical axis. In addition, the 110 K filter triangular groove structure cannot be implemented as BOR. Therefore, the AR coating has been implemented with appropriate dielectric constant slabs on each side of the 5 mm PTFE layer. Firstly, to compare these results with those in the previous HFSS analysis (which included offsets and tilt angles in the IR filters), the feed horn has been simulated with IR filter rims and dielectrics only. The schematics of these simulations

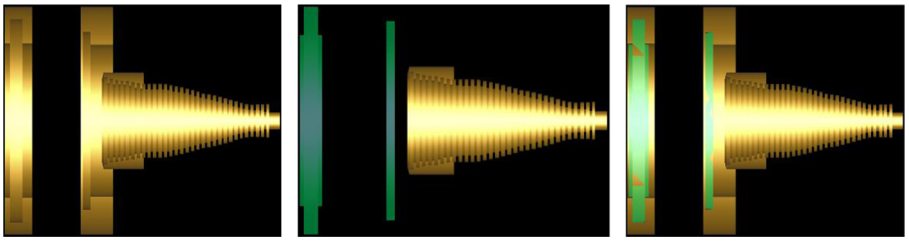

Fig. 9 Schematics of the BOR simulations of ALMA band 1 corrugated horn and IR filters. From left to right, with only metal rims, with only dielectrics, and with the full IR filter assemblies

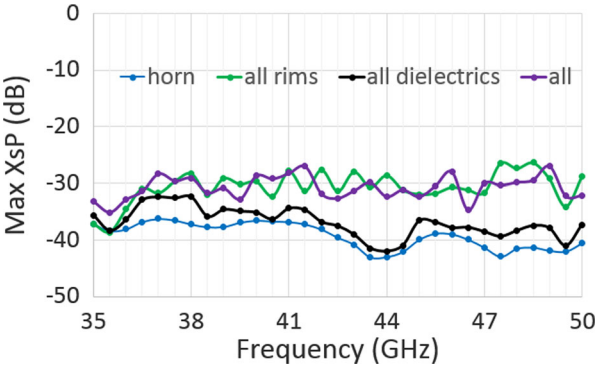

Fig. 10 Results of maximum cross-polarization for different combinations of corrugated horn and BOR models of IR filters. These results represent the same performance as in Fig. 8 but with a different modeling of the IR filters and with a different electromagnetic simulation method

are shown in Fig. 9. Results of cross-polarization analysis are shown in Fig. 10. Qualitative results are similar to those with HFSS shown in Fig. 8. However, the exact frequency behavior is different due to the slightly different geometry.

The next step in the analysis is the inclusion of the lens and its rim in the BOR simulations. The schematic of the full ALMA band 1 optics BOR model is shown in Fig. 11. Results of simulations are shown in Fig. 12. One important qualitative result clearly stands out: the aperture efficiency is degraded in average when any elements of the IR filters are included in the simulation. The changes shown in co- and cross-polarization feed horn fields make that the band 1 lens does not illuminate the secondary mirror of the Cassegrain antenna as designed. In addition, the complex frequency behavior of the input admittance seen at the horn aperture creates ripples in the different efficiencies. These ripples depend on the exact position and material properties of the filters and can cause deep performance degradation over relatively narrow frequency ranges. Sudden aperture efficiency changes in the order of 1.5% can be found within 1 GHz in the performed

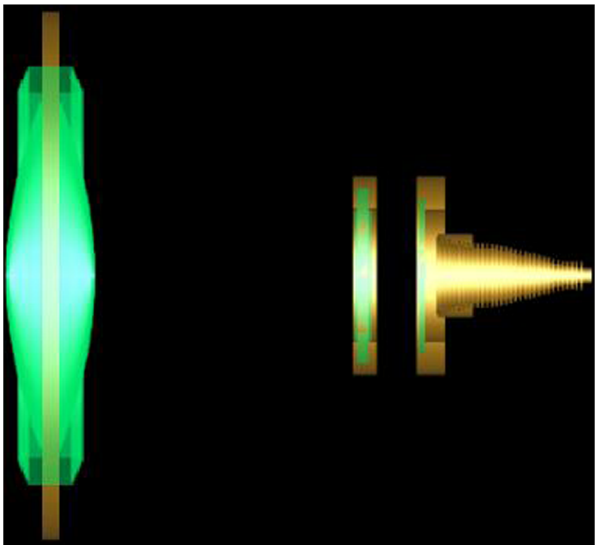

Fig. 11 WaspNET schematic for the simulation of ALMA band 1 optics including BOR models of IR filters

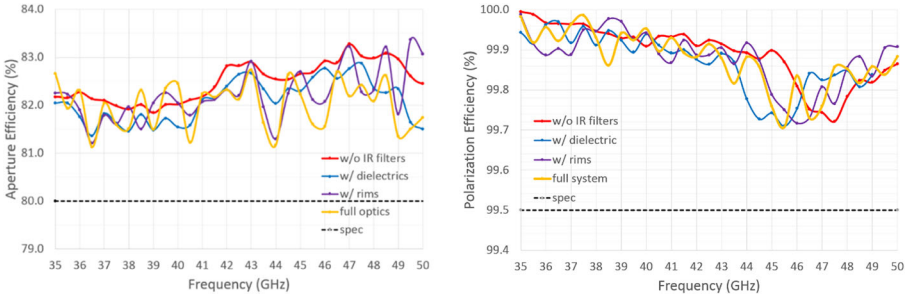

Fig. 12 Aperture efficiency and polarization efficiency for ALMA band 1 optics with and without BOR models of IR filters

simulations. Polarization efficiency can also be degraded sharply as seen in the dip at around 45 GHz in Fig. 12. For the nominal positions of filters and for these qualitative simulations, aperture efficiency does not degrade beyond 81% for ideal components. Fabrication errors and the effects of the real geometry could bring efficiencies close to or even below specifications at some frequencies.

As explained above, the exact frequency behavior of the ripples in efficiencies will depend on the input admittance seen by the horn. Small changes in the positions of IR filters will therefore change the exact frequency behavior of the different efficiencies. This has been confirmed by WaspNET BOR simulations, as presented in Fig. 13. The positions of ripples change under different conditions in a complex manner. Notice that some frequencies, e.g., 41 and 43 GHz, do not show changes in aperture efficiency, whereas other, e.g., 46 GHz, show changes larger than 2% and strongly depend on the position of the IR filters. Unfortunately, there are no tight tolerances on the position of IR filters in the ALMA cryostat, and therefore, performance is expected to change for the different front ends due to these effects.

4 Cryogenic Measurements

ALMA band 1 receivers will be operated in cryogenic and vacuum conditions. So far, measurements reported in [5] showed the performance of the designed optics, measured in a laboratory test bench without IR filters. As described in the previous sections, different

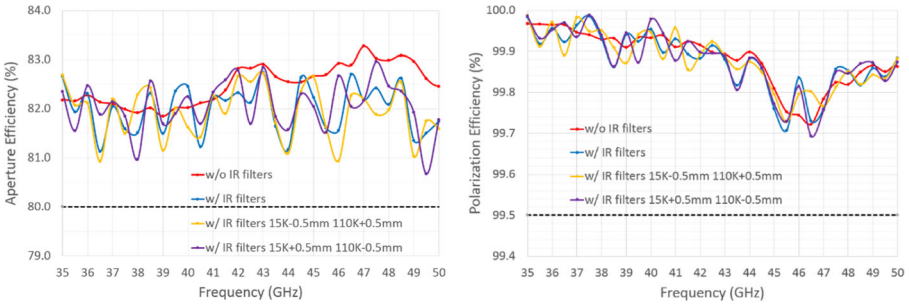

Fig. 13 Aperture efficiency and polarization efficiency variations for different positions of IR filters

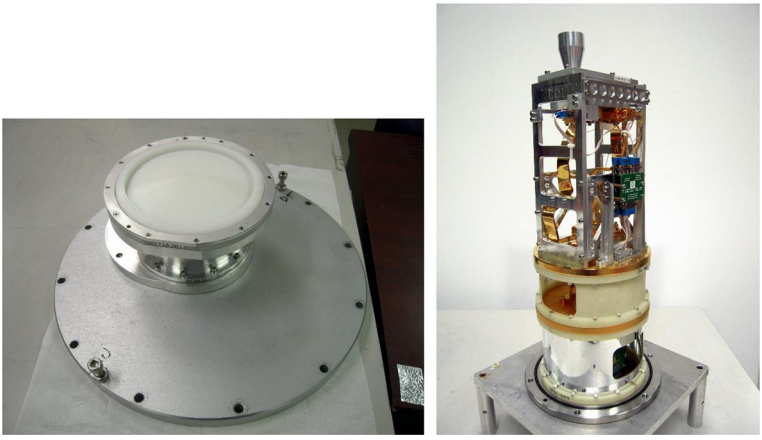

Fig. 14 *Left* band 1 HDPE lens assembled on support structure on top of the ALMA test cryostat top plate. *Right* band 1 CCA, with the corrugated feed horn clearly visible on top

receivers will show slightly different performance due to tolerances and will suffer from the effects of IR filters in real operation conditions inside the cryostat. This latter effect will degrade the average aperture efficiency by around 1%, and with peak degradations approaching (or going below) the 80% aperture efficiency ALMA specification. Effects on polarization efficiency are qualitatively similar, with the possibility of deep degradation peaks as reported for ALMA band 4 [13]. For both efficiencies, large variations are expected at the upper end of the band, close to 50 GHz. In addition, the HDPE lens will be the vacuum seal for the ALMA cryostat and some minor deformations in the order of tenths of millimeters are expected. This will slightly change the performance of the designed optics.

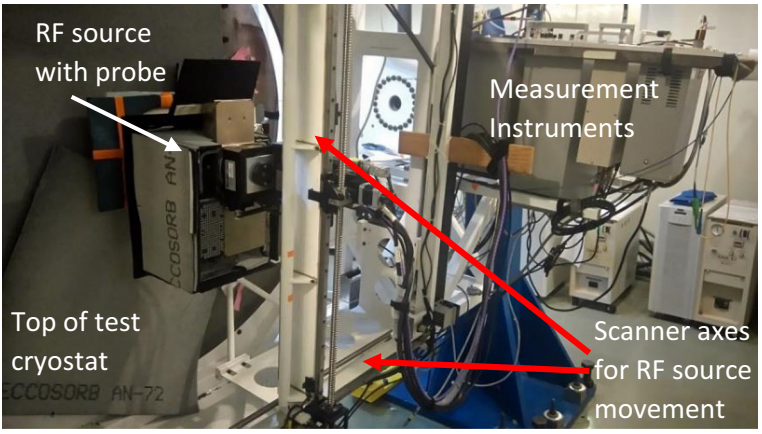

Fig. 15 Near-field beam measurement system for cryogenic measurements. The receiver is placed inside a test cryostat installed on a large tilt table. The top of the cryostat is covered with Eccosorb AN-72 absorber to avoid reflections. The RF source with the probe antenna is placed close to the ALMA band 1 lens and also covered with absorber. The RF source is mounted on two orthogonal movement axes and an extra axis for rotation. Instruments are placed near the scanner to avoid long RF cables

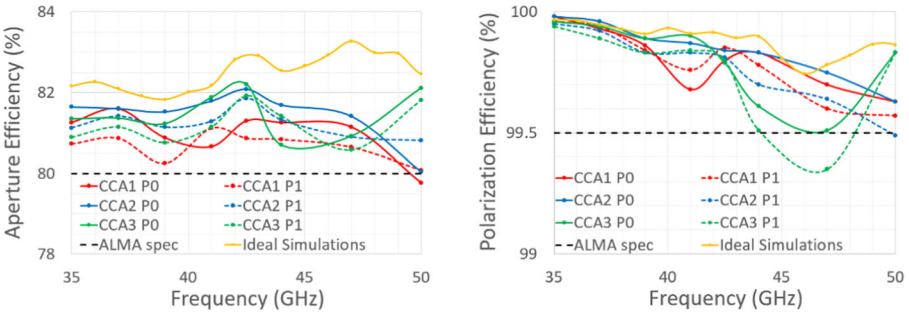

Fig. 16 Measured efficiencies for orthogonal linear polarizations P0, P1 for the first 3 ALMA band 1 receivers at cryogenic temperature. Results of ideal simulations without tolerances and IR filter effects are presented for comparison

Three ALMA band 1 receivers (Cold Cartridge Assembly (CCA)) have been assembled and fully characterized in the setups which will be used during production of the 73 cartridge receivers necessary for ALMA. The description of the first cartridge receiver can be found in [2]. Photographs of one of the first ALMA band 1 CCAs and the lens assembled on top of the cryostat top plate are presented in Fig. 14. The ALMA band 1 optics point at azimuth = 0°, elevation = 2.48° in this configuration. The measurement

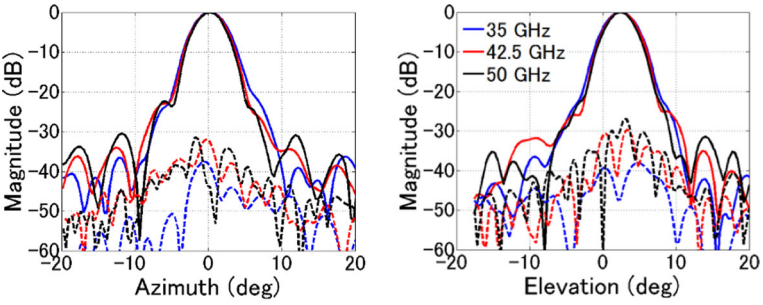

(a) Polarization P0

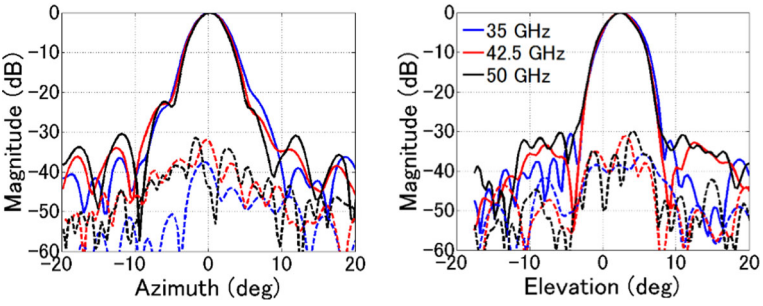

(b) Polarization P1

Fig. 17 Comparison of radiated fields at three different frequencies, 35, 42.5, and 50 GHz for CCA 1. Co-polarization patterns are shown in *solid line* and cross-polarization patterns in *dashed line*. The nominal pointing angle is azimuth = 0°, elevation = 2.48°

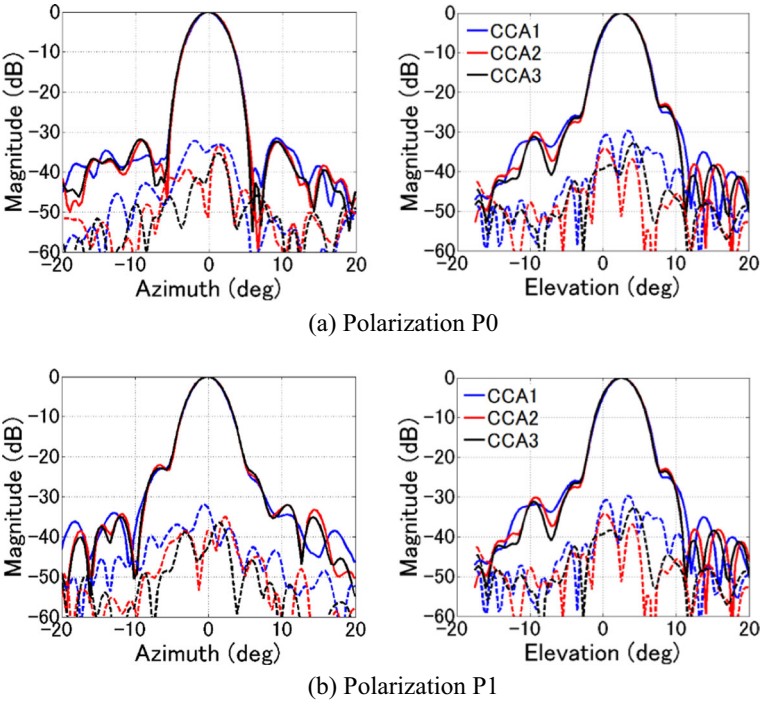

Fig. 18 Comparison of radiated fields at 42.5 GHz for the first 3 ALMA band 1 receivers (CCA 1 to 3). Co-polarization patterns are shown in *solid line* and cross-polarization patterns in *dashed line*. The nominal pointing angle is azimuth = 0°, elevation = 2.48°

setup uses a large tilt table with a cryostat installed in it. This allows characterization of the full receiver with different elevation orientations, to re-create real operation in ALMA antennas. For these tests, all measurements are with zero tilt angle, with the receiver in horizontal position. The probe antenna and source are placed on two moving and one rotation axes. This allows to change the relative position of the probe and the receiver on a plane in front of the receiver and parallel to the top plate of the cryostat, in order to acquire near-field patterns. This is shown in Fig. 15. Measured near-field patterns are then transformed to far fields after applying probe compensation and measurement plane planarity compensation procedures [15]. Optical efficiencies are calculated using ALMA qualified software.

Results of the efficiency analysis of measurements for the first three ALMA band 1 receivers, with a frequency spacing of around 2 GHz, are shown in Fig. 16. As expected from the results in previous sections, the performance is slightly different for the three receivers. In particular, we can see the large variations of aperture efficiency at 50 GHz, and the different values of polarization efficiency at some particular frequencies, presumably determined by the position of the IR filters in the test cryostat. Performance is mostly compliant with the stringent ALMA specifications, except for some slight degradation at particular frequencies, which were expected as explained above. In any case, the non-compliances are minor and dependent on the particular test cryostat. A different test cryostat with different IR filter positions due to tolerances would render slightly different results. A comparison of beam pattern principal plane cuts is presented for CCA1 at three different frequencies and for two orthogonal linear

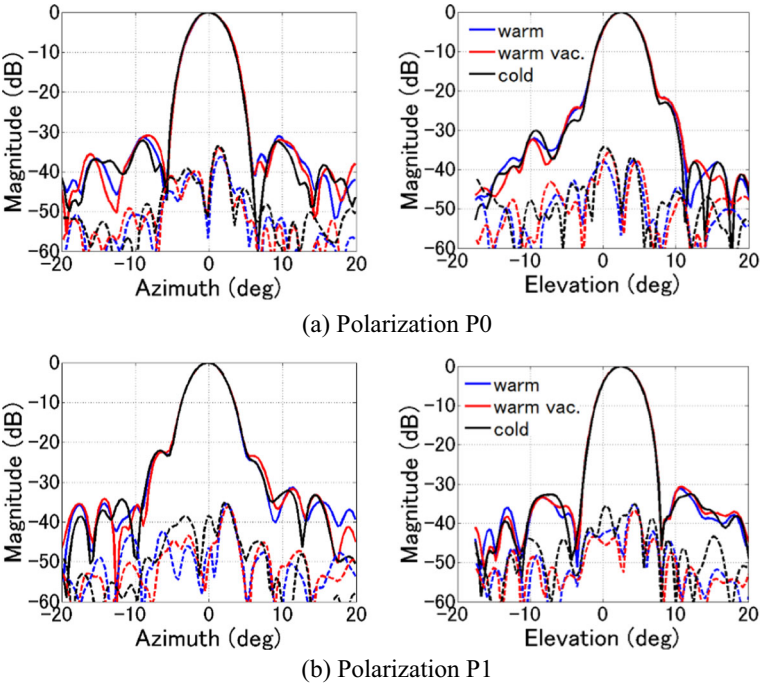

Fig. 19 Comparison of radiated fields at 42.5 GHz for CCA 2 in different operation conditions: warm, after creating vacuum, and after cooling down to 15 K. Co-polarization patterns are shown in *solid line* and cross-polarization patterns in *dashed line*. The nominal pointing angle is azimuth = 0°, elevation = 2.48°.

polarizations in Fig. 17. Beams are very similar in the angular range under which the ALMA secondary mirror is seen (±3.57°). Differences in side-lobes and cross-polarization are related to fabrication tolerances and the different effects of IR filters on particular horn antennas. Figure 18 shows the comparison of far field patterns for the 3 CCAs at 42.5 GHz. Results are again very similar, which confirms good repeatability of the performance of different receivers. This is important towards the production of 73 receivers for ALMA. Finally, Fig. 19 shows the effect of different operating conditions on the CCA 2 beam patterns. Firstly, patterns were measured with the receiver inside the cryostat but at room temperature and pressure. Then, measurements were repeated at room temperature after creating vacuum, and after cooling down the receivers to 15 K. Results show minor changes in cross-polarization and side-lobes, with the central part of the main beam mostly unchanged. Table 1 shows the results of efficiency analysis for these cases at 42.5 GHz.

Table 1 Comparison of aperture and polarization efficiencies at 42.5 GHz for CCA 2

	Aperture efficiency (%)		Polarization efficiency (%)	
Polarization	P0	P1	P0	P1
Warm (no vacuum)	81.70	81.75	99.86	99.80
Warm (vacuum)	81.65	81.50	99.82	99.81
Cold (vacuum)	82.09	81.86	99.84	99.81

5 Conclusions

In this paper, we have analyzed the effects of component fabrication errors and real operating conditions on the performance of the highly optimized ALMA band 1 optics design presented in [5]. The results of these analyses show that performance of up to 73 ALMA band 1 receiver optics is expected to be mostly compliant with ALMA specifications. Minor non-compliances are possible due to the combined effects of fabrication errors and IR filter effects. These conclusions have been confirmed with the beam measurement characterization of the first three ALMA band 1 receivers at cryogenic temperature. Performance of the first three produced receivers is compliant with ALMA specifications. Slight non-compliances are related to the measurement setup and will potentially differ when receivers are tested or operated in different cryostats with different IR filter positions. The results of this paper are of interest for the design of mm-wave quasi-optical systems using dielectric lenses, especially if expected to be operated at cryogenic temperature or under vacuum conditions.

References

1. A. Wootten, and A. Thompson, “The Atacama Large Millimeter/Submillimeter Array,” Proceedings of the IEEE, vol.97, 1463 (2009)
2. Y-J. Hwang, et al., “Band 1 receiver front-end cartridges for Atacama Large Millimeter/submillimeter Array (ALMA): design and development toward production”, SPIE conference on Astronomical Telescopes + Instrumentation 2016 (2016)
3. N. Reyes, et al., “Design of the optical system for ALMA Band 1,” in Proceedings of SPIE Vol. 9145, p. 91451W (2014)
4. A. Gonzalez, et al., “Alternative optics design for the ALMA Band 1 receiver (35–52 GHz),” in European Conference on Antennas and Propagation (EuCAP), pp. 1–4 (2015).
5. V. Tapia, et al., “High Efficiency Wideband Refractive Optics for ALMA Band-1 (35-52 GHz)”, Journal of Infrared, Millimeter, and Terahertz Waves, Vol. 38, Issue 3, pp. 261–275 (2017)
6. J. M. Hammersly and D. C. Handscomb, Monte Carlo Methods. New York: Wiley, 1964.
7. A. Gonzalez, and Y. Uzawa, “Tolerance Analysis of ALMA Band 10 Corrugated Horns and Optics”, IEEE Transactions on Antennas and Propagation, Vol. 60, No. 7, pp. 3137–3145, 2012
8. A. Hammar, M. Whale, P. Forsberg, A. Murk, A. Emrich, and J. Stake, “Optical Tolerance Analysis of the Multi-Beam Limb Viewing Instrument STEAMR”, IEEE Transactions on Terahertz Science and Technology, Vol. 4, No. 6, pp. 714–721, 2014
9. M. Candotti, Y. Uzawa, S. V. Shitov, Y. Fujii, and K. Kaneko, “ALMA band 10 optics tolerance analysis,” in Proc. 19th Int. Symp. on Space THz Technol., Groningen, The Netherlands, 2008, pp. 521–527
10. MIG WASP-NET, software description. Available: http://www.mig-germany.com/
11. MathWorks MATLAB, software description. Available: https://www.mathworks.com/products/matlab.html
12. A. Gonzalez, S. Asayama, V. Tapia, R. Finger, D. Monasterio and N. Reyes, "Effects of cryostat infrared filters on the performance of ALMA band 1 (35–52 GHz) receiver optics," 2016 I.E. International Symposium on Antennas and Propagation (APS-URSI), Fajardo, 2016, pp. 381–382
13. A. Gonzalez, and Y. Uzawa, “Investigation on ALMA Band-4 Frequency-Dependent Cross-Polarization”, IEEE Transactions on Terahertz Science and Technology, Vol. 4, Issue 2, pp.184–192 (2014)
14. ANSYS HFSS, software description. Available: http://www.ansys.com/products/electronics/ansys-hfss
15. D. Slater, Near-Field Antenna Measurements. Norwood: Artech House, 1991